Effects of a Groundwater Scheme on the Simulation of Soil Moisture and Evapotranspiration over Southern South America

J. ALEJANDRO MARTINEZ[a]

Department of Atmospheric Sciences, The University of Arizona, Tucson, Arizona

FRANCINA DOMINGUEZ

Department of Atmospheric Sciences, University of Illinois at Urbana–Champaign, Urbana, Illinois

GONZALO MIGUEZ-MACHO

Faculty of Physics, Universidad de Santiago de Compostela, Galicia, Spain

(Manuscript received 25 February 2016, in final form 27 September 2016)

ABSTRACT

The effects of groundwater dynamics on the representation of water storage and evapotranspiration (ET) over southern South America are studied from simulations with the Noah-MP land surface model. The model is run with three different configurations: one including the Miguez-Macho and Fan groundwater scheme, another with the Simple Groundwater Model (SIMGM), and the other with free drainage at the bottom of the soil column. The first objective is to assess the effects of the groundwater schemes using a grid size typical of regional climate model simulations at the continental scale (20 km). The phase and amplitude of the fluctuations in the terrestrial water storage over the southern Amazon are improved with one of the groundwater schemes. An increase in the moisture in the top 2 m of the soil is found in those regions where the water table is closer to the land surface, including the western and southern Amazon and the La Plata basin. This induces an increase in ET over the southern La Plata basin, where ET is water limited. There is also a seasonal increase in ET during the dry season over parts of the southern Amazon. The second objective is to assess the role of the horizontal resolution on the effects induced by the Miguez-Macho and Fan groundwater scheme using simulations with grid sizes of 5 and 20 km. Over the La Plata basin, the effect of groundwater on ET is amplified at the 5-km resolution. Notably, over parts of the Amazon, the groundwater scheme increases ET only at the higher 5-km resolution.

1. Introduction

In spite of the tremendous advances in the representation of many processes in land surface models (LSMs), the simulation of the storage (e.g., soil moisture) and fluxes of moisture [e.g., evapotranspiration (ET)] requires further improvement. Koster et al. (2009, p. 4334) state that "it is possible that land surface models are, indeed, all 'wrong in precisely the same way,' reducing their usefulness for such a real-world application. For example, they all lack, to some degree, sophisticated treatments of certain hydrological processes (e.g., baseflow, interflow), and most share similar simple representations of other hydrological processes." In the case of South America, Chen et al. (2010) found that Global Land Data Assimilation System (GLDAS)-Noah does not give an account of some of the amplitude of the monthly-scale fluctuations in the terrestrial water storage (TWS) field over the southern La Plata basin, maybe because of the lack of a representation of groundwater processes. Ferreira et al. (2011) found that GLDAS-Noah and WRF-Noah both underestimate soil moisture over northeastern Argentina. From the simulation of the water balance of the Amazon basin with 14 LSMs, Getirana et al. (2014) also suggest that there are still several aspects where the LSMs need improvement, in particular the simulation of ET.

One fundamental component affecting soil moisture dynamics is the distribution of shallow groundwater

[a] Current affiliation: Institute of Physics, University of Antioquia, Medellin, Colombia.

Corresponding author address: Francina Dominguez, Department of Atmospheric Sciences, University of Illinois at Urbana–Champaign, 105 S. Gregory St., Urbana, IL 61801-3070.
E-mail: francina@illinois.edu

DOI: 10.1175/JHM-D-16-0051.1

(Fan et al. 2013; Fan 2015). Shallow unconfined aquifers have an effect on the content of moisture in the layers closer to the land surface (e.g., the critical zone), as the downward flux (drainage) can be reduced and even reversed by the presence of groundwater. In addition, where groundwater is shallow, or where roots are deep enough, the groundwater can directly be used by plants, affecting the land surface fluxes of moisture and energy via effects on transpiration (Fan 2015). By studying the water balance components measured on an Amazonian microcatchment, Tomasella et al. (2008) found strong memory features of the groundwater component in the form of anomalies that persist on the scale of years. The authors suggest that the memory of the groundwater affects the moisture content in the unsaturated zone and ET, which are very important for understanding the variability of the weather and climate of the region. Pfeffer et al. (2014) estimated the depth of the water table for the central Amazon using satellite data for the period 2003–08. They also found strong memory features at the basin scale, in particular in the response of the central Amazon to the drought of 2005: the negative anomalies in the water table persisted until 2007. Studying the Argentine Pampas (southern La Plata basin), Kuppel et al. (2015) found significant correlations between the water-table depth and TWS and between TWS and ET. There is also a monotonic relationship between the water-table depth and the surface water cover. Thus, groundwater in this region is also a critical factor for flood dynamics and ET anomalies. In the modeling study by Chen et al. (2010), the authors found a better representation of the fluctuations of TWS when they combined the GLDAS-Noah data with groundwater observations over the southern La Plata basin.

Given its importance for surface hydrology, and its corresponding impact on the fluxes of energy and moisture at the land–atmosphere interface, schemes to represent groundwater processes and water-table dynamics have been developed in the last 10–15 years as new components of LSMs for weather and climate studies. Niu et al. (2007) found that a groundwater scheme increased the simulated soil moisture and ET over parts of South America, including the southern half of the Amazon basin, the western La Plata basin, and northeastern Brazil. Miguez-Macho and Fan (2012b) estimate that the water table is less than 2 m deep over 20%–40% of the Amazon basin. The shallow groundwater reduces drainage during the wet season and even supports capillary rise over parts of the Amazon during the dry season; both effects increase dry season soil moisture and ET. In the third paper of that series, Pokhrel et al. (2013) also find a better agreement with TWS from Gravity Recovery and Climate Experiment (GRACE) when the dynamic groundwater is included. Koirala et al. (2014) found an improvement in the simulation of the discharge of the Amazon River (in phase and amplitude).

Shallow water tables are found not only in the Amazon basin, but also in other parts of South America, and in particular in the La Plata basin (Fan and Miguez-Macho 2010; Fan et al. 2013). This suggests that groundwater dynamics might have an important role on the water balance and its variability over this region. Furthermore, given the strong land–atmosphere coupling in southern South America (see, e.g., Collini et al. 2008; Sörensson and Menéndez 2011; Dirmeyer et al. 2009), the representation of groundwater dynamics on LSMs might also have potential impacts on the simulation of the atmospheric processes, including precipitation. Consequently, there is a critical need to study the role of groundwater on the water balance over central and southern South America.

The goal of this study is to explore the effects of a groundwater scheme on the simulation of moisture storage and fluxes over a region that includes the southern Amazon and La Plata basins. Specifically, we ask 1) what are the spatial and seasonal differences in the simulation of TWS, soil moisture, and ET when a groundwater scheme is included and 2) what is the effect of the horizontal resolution of the groundwater scheme on the simulation of ET? To address the first question, we perform 10-yr simulations in offline mode (i.e., with prescribed atmospheric conditions) using a grid size of 20 km. We compare simulations that use the groundwater schemes developed by Miguez-Macho et al. (2007) and Niu et al. (2007) with a simulation that has free drainage as boundary condition at the bottom of the resolved soil layers. We assess the effects of the groundwater by comparing the TWS, soil moisture, and ET in both simulations, with a focus on features at the regional scale. To address the second question, we perform simulations with and without the Miguez-Macho and Fan (MMF) scheme, with grid sizes of 20 and 5 km. While the results of simulations with 20-km grid size are relevant for the interpretation of current climate simulations, the comparison of the lower- and higher-resolution simulations provide a picture of those regions where higher resolution or additional parameterizations are needed.

2. Methodology

a. *Region of study*

The model domain includes parts of the La Plata basin (LPB), the southern half of the Amazon basin, and central-eastern Brazil (Fig. 1). The LPB extends over parts of five countries, is the second-largest system in

South America, and its water resources are a key component of the economy of the region, which is one of the most densely populated areas in South America (Berbery and Barros 2002). The southern Amazon and central-eastern Brazil play important roles in the local and regional climate, in particular because of its connection with the South American monsoon system (e.g., Marengo et al. 2012; Collini et al. 2008; Vera et al. 2006) and the transport of water vapor to the La Plata basin (e.g., Marengo et al. 2004; Martinez and Dominguez 2014).

b. The MMF groundwater scheme

In the present study, we use the groundwater scheme developed by Miguez-Macho et al. (2007), as currently implemented in the Noah-MP LSM (Barlage et al. 2015). The MMF scheme includes a representation of the interaction of the shallow groundwater with the unsaturated zone by adding an unconfined aquifer below the lowest resolved soil layer. The water balance for this aquifer includes the interaction with the unsaturated zone (vertical fluxes) and with the river network (horizontal fluxes). The vertical fluxes represent the gravitational drain and the capillary fluxes, and Darcy's law is used to represent the resulting flux. There is also an explicit representation of the lateral movement of the groundwater, given by the horizontal flow between each grid cell and its eight neighboring grid cells. These fluxes are estimated via Darcy's law with the Dupuit–Forchheimer approximation (Fan and Miguez-Macho 2010). Lateral flow between the groundwater and the river network is also represented by a Darcy's law–type equation. The boundary condition for the water-table depth is set at sea level along the coasts and at equilibrium values in continental areas. Missing the relatively small variations of the water-table depth along the continental boundary cells has a negligible impact on the results, except on the vicinity of these grid cells, because of the slow lateral propagation of the errors at the resolution used in this study.

c. The Simple Groundwater Model

The Simple Groundwater Model (SIMGM; Niu et al. 2007) as incorporated in Noah-MP (Niu et al. 2011) is also used in this study. In this scheme, an unconfined aquifer is added below the resolved soil layers. The water balance of this reservoir depends on the recharge rate Q (exchange with the soil layers above) and the discharge rate R (which is a lateral flow). Recharge rate is parameterized using Darcy's law and thus depends on the water-table depth [see Eq. (6) in Niu et al. (2007)]. In turn, the water-table depth is updated depending on Q. Discharge rate is parameterized using TOPMODEL concepts. This means that the lateral flow is not explicitly resolved as in the MMF scheme (Niu et al. 2007). In addition, some parameters in the SIMGM scheme come from global averages (Niu et al. 2011), while more information of the local topography is incorporated into the parameters of the MMF scheme (Miguez-Macho et al. 2007).

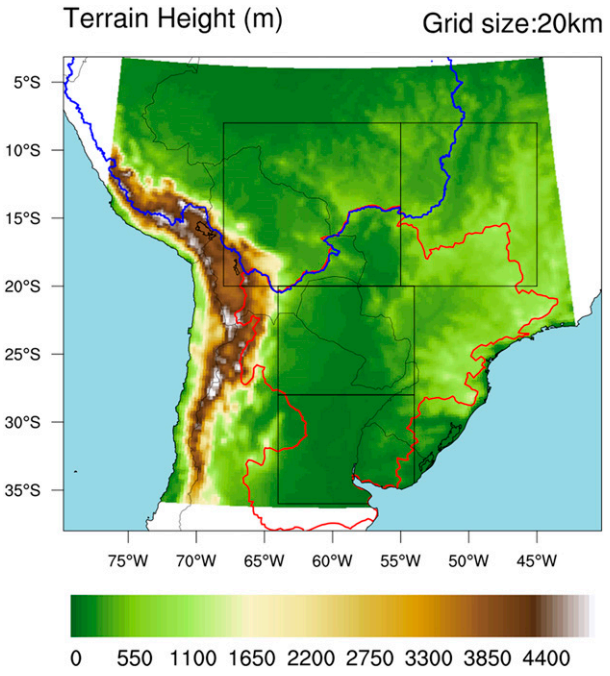

FIG. 1. Model domain and topography at 20-km grid size. Red contour represents the LPB. Blue contour represents the Amazon basin.

d. Model configuration

This study uses the Noah LSM with multiparameterization options (Noah-MP; Niu et al. 2011). We use the Noah-MP, version 1.6 (which is also included within WRF, version 3.6), in offline mode (i.e., with prescribed atmospheric conditions). We run the model at two different grid sizes (20 and 5 km, see details below), with a time step of 30 min (see, e.g., Getirana et al. 2014). We have modified the soil column to have 14 layers extending from the land surface to 4 m below, using the same configuration as Miguez-Macho and Fan (2012a). The rooting depth is the same as in the default Noah-MP and Noah models [e.g., see Fig. 1 and Table 1 in Sörensson and Berbery (2015)]. It is important to highlight that the maximum rooting depth in Noah-MP is currently 2 m, despite the fact that roots can extend much deeper, with reports of 18-m-deep roots in the Cerrado of Brazil (Rawitscher 1948).

Following the studies by Miguez-Macho and Fan (2012a,b), which also use the MMF scheme for a region over South America, and in order to compare our results with these studies, we use initial conditions and

atmospheric forcing from the ERA-Interim archive (Dee et al. 2011). This reanalysis has some known biases over South America (Betts et al. 2009). Compared to the observation-based forcing fields of the GLDAS, version 1, product (Rodell et al. 2004), ERA-Interim has a negative bias in downward shortwave radiation and a positive bias of precipitation over parts of our domain (not shown). In this study we focus on the differences between different model configurations, namely, with and without a groundwater scheme, and the role of the horizontal resolution. Since the ERA-Interim biases are likely to affect our simulations with different model configurations in a similar way, the differences between simulations are expected to be mostly due to the model configurations. Our subsequent study with a coupled land–atmosphere system (WRF-Noah-MP; Martinez et al. 2016) supports this hypothesis.

e. *Assessing the role of the groundwater*

To assess the effects of the representation of the groundwater dynamics in the Noah-MP LSM, we run the model with three different configurations. In the first configuration, the MMF groundwater scheme (Miguez-Macho et al. 2007) is activated; we will refer to simulations with this configuration as the groundwater (GW) simulations. In the second configuration, the soil moisture is allowed to drain freely from the bottom layer of the soil column under the action of gravity solely, that is, no interaction with a groundwater reservoir is taken into account; we will refer to simulations with this configuration as the free drainage (FD) simulations. The third configuration uses the groundwater scheme developed by Niu et al. (2007); in this way we obtain our SIMGM simulations. The offline simulations are a first step that will help us later to interpret fully coupled land–atmosphere simulations at horizontal resolutions that are typical of continental-scale regional climate modeling studies over South America (e.g., Solman et al. 2013; Lee and Berbery 2012; Müller et al. 2014) and that could affect the state of the atmosphere (e.g., affecting precipitation). For this reason, we seek regional-scale patterns of soil and land surface conditions induced by the groundwater schemes using simulations with a grid size of 20 km.

The slowest component of our simulations is the groundwater scheme, demanding multiple years of spinup. Both groundwater schemes are initialized independently, starting from their equilibrium conditions as obtained in previous studies (Fan and Miguez-Macho 2010; Niu et al. 2011). A first simulation of 20 years (1994–2013) is performed for each configuration. The final state and some parameters are then used again for a second 20-yr simulation for the same period. For each scheme we restrict our analysis to the 10-yr period 2004–13 of the second simulation. Therefore, the approximate spinup is 30 years (20 years from the first simulation, and 10 years from the second simulation). Because the FD simulation does not include a groundwater component, and in order to isolate the effects of different initial conditions in the comparison of the GW and FD simulations, we use the same initial conditions for the FD simulation as for the second 2004–13 GW simulation [similar to Anyah et al. (2008)].

f. *Assessing the role of the horizontal resolution: 20- versus 5-km simulations*

The second objective of the present study is to assess the sensitivity of the effects of the MMF groundwater scheme to the horizontal resolution of the model. We run a second set of simulations that include two runs with a grid size of 20 km (GW20 and FD20) and two runs at 5-km grid size (GW05 and FD05). All simulations start from the same initial condition on 1 December 2003 and run through 31 December 2007. The initial conditions for the MMF scheme come from equilibrium calculations with a grid size of approximately 274 m (Fan and Miguez-Macho 2010). For the present simulations no spinup is considered (except for excluding the first month of simulation from the analysis). The focus is on the difference between two spatial resolutions, that is, differences of the type (GW05 − FD05) versus (GW20 − FD20). This analysis has to be interpreted carefully because of the lack of spinup for each resolution separately. By computing the differences at the same grid size first and then comparing both resolutions (instead of comparing directly the groundwater schemes at two different resolutions, e.g., GW05 − GW20), we hope to get a better idea of the effect of the groundwater scheme at higher resolutions, filtering in this way part of the effect of the lack of spinup and the effect of the grid size alone. This expectation is somewhat met as suggested by steady character of our results (see below).

Table 1 presents a summary of some of the model simulations.

3. Results

a. *Effects of the groundwater schemes with grid size of 20 km*

Over most of the domain, the rainy season is from October–November through March–April (Fig. 2, top). The dry season peaks in July–August. To facilitate our analysis, we define four regions of interest: the southern

TABLE 1. Configurations of the simulations with the Noah-MP LSM in offline mode. GW (SIMGM) denotes simulations with the MMF (SIMGM) groundwater scheme. FD denotes simulations with free drainage. The soil column will have 14 layers, with bottom at 4 m, for all simulations.

Expt	Grid size (km)	Period
GW	20	2004–13
SIMGM	20	2004–13
FD	20	2004–13
GW05	5	2004–07
FD05	5	2004–07
GW20	20	2004–07
FD20	20	2004–07

Amazon (SOAM; 20°–8°S, 68°–55°W), the South American monsoon region [SAMS; 20°–8°S, 55°–45°W; similar to Collini et al. (2008)], the upper La Plata (UPLP; 28°–20°S, 64°–54°W), and the lower La Plata (LOLP; 36°–28°S, 64°–54°W). The amplitude of the precipitation cycle is larger for the monsoon region, while the southern Amazon receives some precipitation even during the dry season. Mean precipitation over the La Plata basin is less than over the north of the domain. While over the southern La Plata basin precipitation peaks around October–November, maximum values over the monsoon region are observed around January. These characteristics of the ERA-Interim precipitation are in agreement with the observation-based analysis of Berbery and Barros (2002).

1) WATER-TABLE DEPTH

The water table in the GW simulation is relatively deep compared with the estimates obtained by Fan and Miguez-Macho (2010) and Fan et al. (2013) (Fig. 2, middle). Over the UPLP and LOLP regions, the water table is mostly below 5-m depth, with some regions above 4-m depth (i.e., where the water table is within the resolved soil layers). In contrast, Fan et al. (2013) found equilibrium values around 2.5 m for the same region.

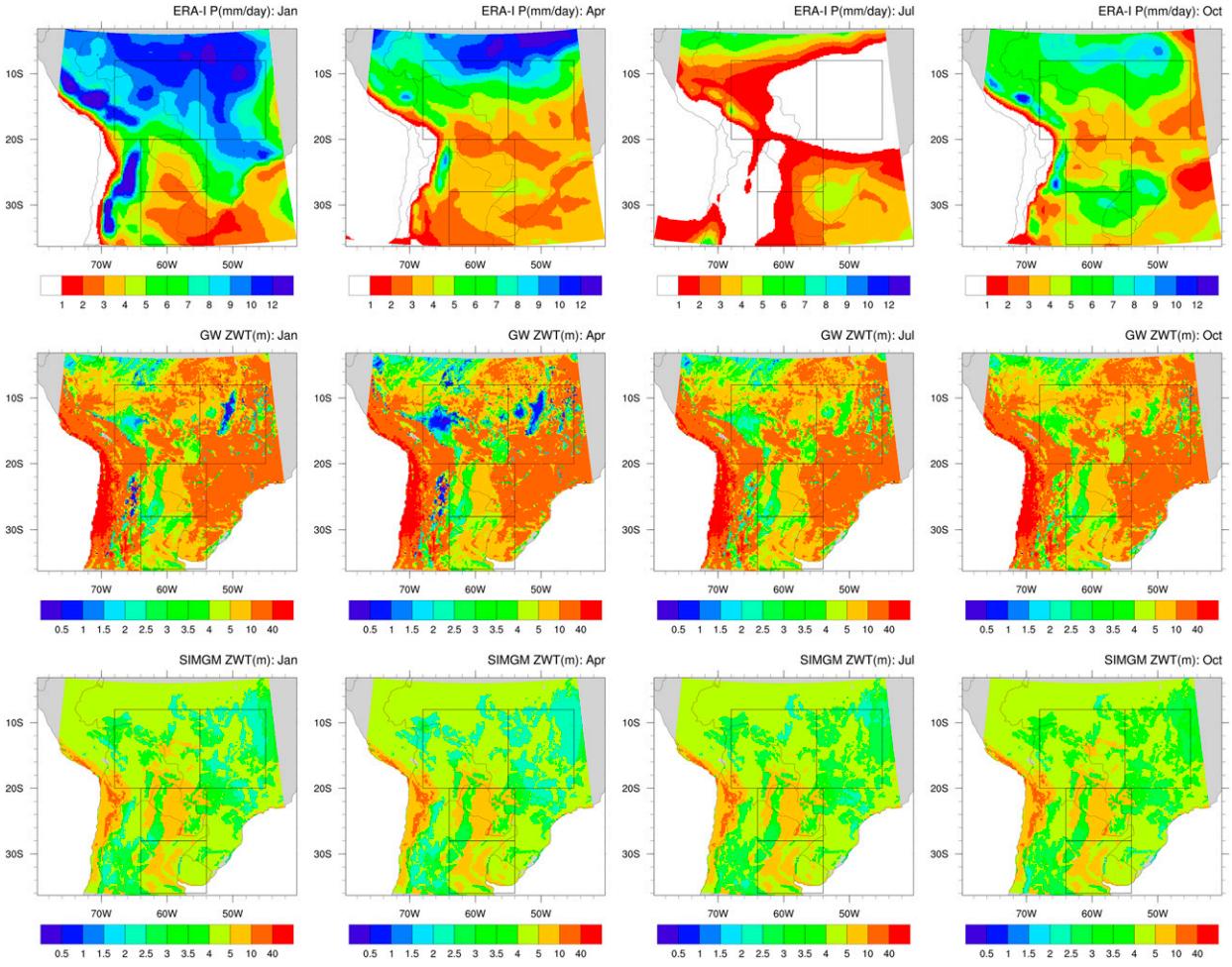

FIG. 2. (top) Mean monthly precipitation from ERA-Interim interpolated to the Noah-MP grid and depth to water table as simulated by the (middle) MMF and (bottom) SIMGM schemes. Grid size is 20 km.

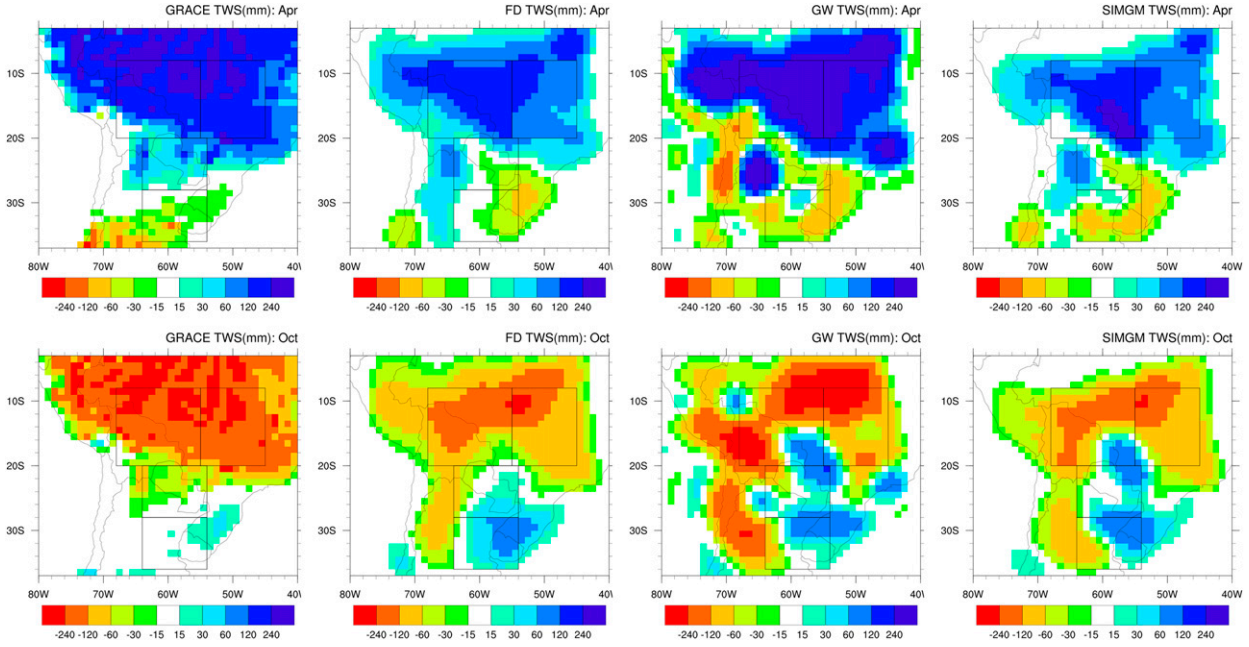

FIG. 3. Seasonal fluctuations in TWS from GRACE and the FD, GW, and SIMGM simulations for (top) April and (bottom) October.

Analogously, the water table over the SOAM and SAMS is deeper than reported by Fan and Miguez-Macho (2010). One major factor contributes to these differences: in this study we are using a much coarser resolution (20 km) compared with Fan and Miguez-Macho (2010) (~270 m) and Miguez-Macho and Fan (2012a,b) (~2 km), which affects the simulation of the lateral movement of the groundwater toward small-scale depressions. However, the GW simulation still shows a relevant fraction of the domain where the water-table depth is within the top 4 m of the soil column (i.e., within the resolved layers). On the other hand, the SIMGM simulation produces a much shallower water table over most of the domain, with values mostly in the 3–5-m range, in agreement with Niu et al. (2007). Figure 2 also shows that there is a seasonal cycle of the water-table depth over parts of the southern Amazon and the monsoon region, with the water-table depth lagging precipitation by nearly 2–3 months.

2) TWS

We estimated the monthly fluctuations in the TWS in both simulations (Fig. 3). For the FD simulation we add the moisture in the canopy and the resolved soil layers (14 levels, bottom at 4 m) to obtain the total water storage. In the MMF scheme (GW simulations) the calculation of the TWS depends on the location of the water-table depth. When the water table is within the resolved soil layers we add the moisture in the canopy, the unsaturated layers, and the water between the water table and a hypothetical bedrock (since our interest is on the fluctuations of TWS, the depth of the hypothetical bedrock does not affect our conclusions). When the water table is below the resolved layers, the MMF scheme explicitly computes the water content in the intermediate layer between the bottom of the resolved layers (at 4 m) and the water-table depth. To obtain the TWS in this case, we add the water in the canopy, the resolved layers, the intermediate layer, and between the water-table depth and the hypothetical bedrock. On the other hand, in the SIMGM scheme the TWS is computed directly by adding the water in the canopy, the resolved soil layers, and the water in the aquifer (G.-Y. Niu 2016, personal communication). The fluctuations in TWS are obtained by subtracting the mean water storage during the base period 2004–09.

For reference, we compare with the fluctuations in TWS from GRACE data (Landerer and Swenson 2012; Swenson and Wahr 2006). The GRACE TWS fluctuations are deviations from the mean value for the 2004–09 period. To compare our simulations to GRACE estimates, we use the same base period for the fluctuations (see above), we regrid our estimates to a 1° grid, decompose our fields in spherical harmonics, and make a T60 truncation, and finally perform a smoothing by doing a nine-point (center and eight neighbors) averaging. This procedure is similar to that by Chen et al. (2010). The large-scale patterns in Fig. 3 are similar among the datasets. Over the north of the domain, the TWS is larger during April, after the end of the rainy

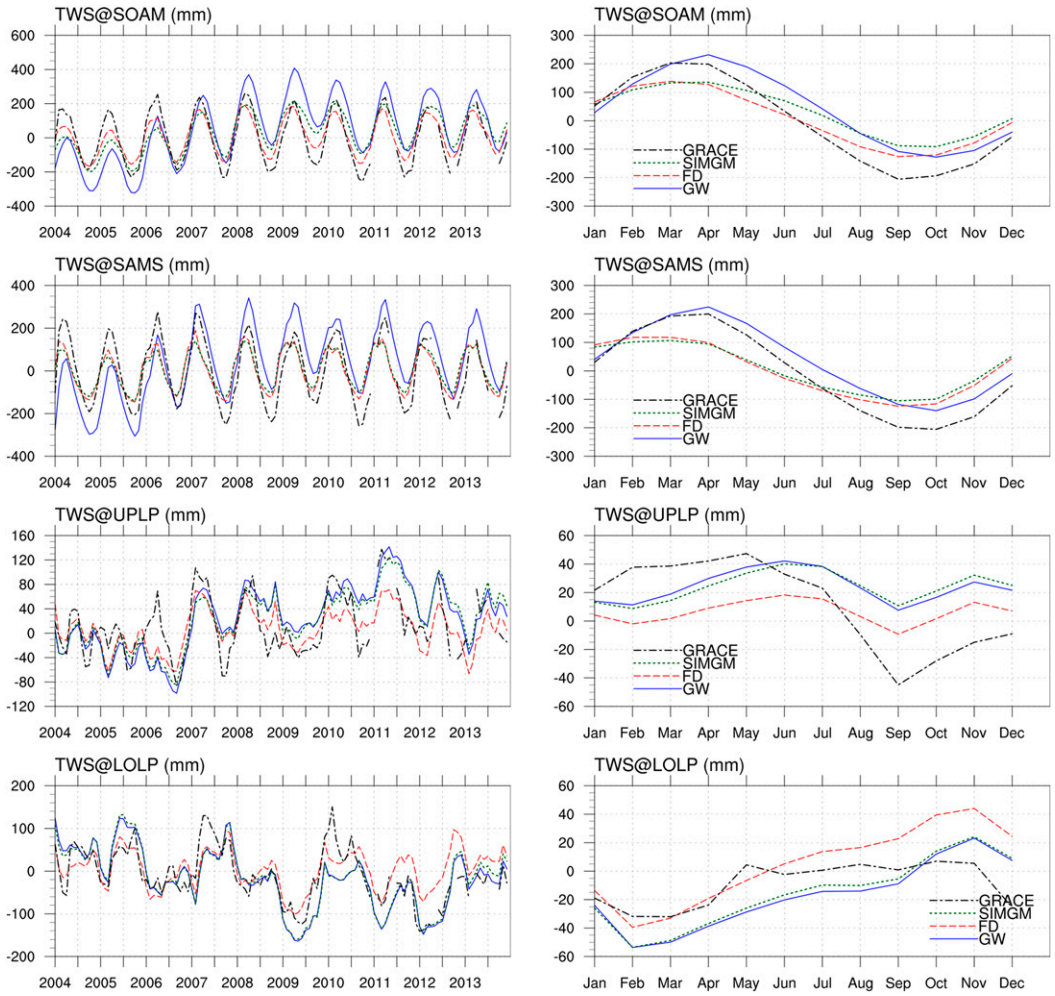

FIG. 4. Monthly fluctuations in TWS averaged over the regions in Fig. 3.

season; then the TWS decreases during the dry season and reaches the lowest values at the onset of the new rainy season. Over the south of the domain (in particular the LOLP region), the highest TWS is seen during the time of minimum precipitation as represented by ERA-Interim (see Fig. 2 and annual cycle of precipitation for LOLP below). Part of the reason seems to be the decrease of ET during the dry winter season, while moisture is still collected from winter precipitation (extratropical systems). Over the north of the domain, the GW simulation more closely resembles the GRACE amplitude during the peak periods April and October. Both the GW and SIMGM simulations show spatial heterogeneities over the south of the domain not present in GRACE. All three simulations show large fluctuations over the Andes, not seen in GRACE.

Both for the southern Amazon and the monsoon region, the GW simulation produces a longer lag in the response of the TWS to the cycle of precipitation (Fig. 4). In the case of the monsoon region (i.e., SAMS) and SOAM, after the first years of simulation, the amplitude in the GW simulation is closer to GRACE than the amplitude of FD. In addition, for the SAMS, the phase of GW is closer to GRACE, whereas the phase of FD is closer to GRACE for SOAM. Thus, the GW simulation seems to produce a better amplitude and phase than FD, even at this "coarse" resolution of 20 km [Pokhrel et al. (2013) found analogous results using ~2 km]. Interestingly, our SIMGM simulation follows closely the behavior of the FD simulation over SOAM and SAMS. The fluctuations in SIMGM are smaller than in GW because in the former the water-table depth is shallower (Fig. 2), which in turn produces smaller variations in soil moisture and moister soils over the north of our domain (see below). Figure 4 shows a jump around 2006 in the TWS for SOAM in the Noah-MP simulations. A similar jump is observed in soil moisture (see below), both in our simulations and in ERA-Interim.

These abrupt changes (in particular in the amplitude of the TWS fluctuations) around 2006 are a result of a jump in the ERA-Interim precipitation over the region, which seems to be an artifact of the reanalysis when compared with TRMM (not shown).

In the case of the La Plata basin, the differences between our simulations and GRACE are more notable. First, note the relatively large year-to-year variability on each time series and how the smaller fluctuations are sometimes out of phase between our simulations and GRACE. Second, the resulting mean annual cycle is noticeably different between our simulations and GRACE, while the simulations are close to each other, in particular GW and SIMGM. The timing of the largest fluctuations seems to be well depicted by our simulations, probably because the variations of the forcing are larger or more relevant than the corresponding biases. This is the case during the drought over the southern La Plata basin between 2008 and 2009 (see, e.g., Chen et al. 2010). Starting around October 2007, all the time series show the same fluctuations throughout 2008 and 2009. One interesting difference is that GW and SIMGM seem to overestimate the rate of decrease in TWS in this period. This decrease seems to have sustained higher values of ET in the simulations with groundwater schemes compared with the FD simulation in response to the lack of precipitation. Finally, note that both the long-term decline and the largest fluctuations of TWS in the GW and SIMGM simulations are more pronounced than in the FD simulation over the southern La Plata basin (i.e., LOLP). In general, our simulations suggest that the groundwater scheme affects the amplitude, phase, and long-term behavior of the fluctuations in TWS.

The largest discrepancies between GRACE and our simulations were found for the UPLP (Fig. 4). In particular, the difference between the first and second half of the year is much smaller in the simulations than in the GRACE estimates, which seems to be associated with an overestimation of the runoff over the UPLP region, which would be unrealistic given the flat terrain and other hydrologic characteristics of the region. The overestimation of runoff is also found in the GLDAS data (not shown). Our hypothesis is that this overestimation arises because the model does not include a flooding scheme [e.g., like the one used by Miguez-Macho and Fan (2012a,b) for the Amazon], despite the fact that a substantial portion of La Plata is in flood-prone areas, wetlands, and marshes, including the Pantanal. These natural storage areas significantly dampen the hydrologic response of the system. Another factor may be the negative bias in precipitation from ERA-Interim during December–May (as compared to TRMM, not shown).

3) SOIL MOISTURE IN THE TOP 2 M

The largest values of soil moisture (Fig. 5) are found over the Amazon (north of the domain), where precipitation is larger (Fig. 2). The amplitude of the seasonal cycle is also larger over this region. The model produces local maxima of soil moisture over southern Brazil and southern La Plata (i.e., LOLP) and intermediate values over the north-central part of the La Plata basin (including UPLP). The differences in moisture between the groundwater (GW and SIMGM) and the FD simulations are positive, which means that the groundwater schemes increase the soil moisture content in the top layers of the soil. This increase is not homogeneous over the domain, but it is larger where the water table is shallower (Fig. 2). Soil moisture in the top 2 m (SM2m) is larger not only in regions where the water table is above the 2-m depth, but also in regions where it is even below the resolved soil layers (4 m). These results show that including a representation of the shallow aquifers reduces the downward flux of soil moisture in the GW and SIMGM simulations compared with the FD simulation. In some regions, the moisture flux can even reverse, going upward from the aquifer to the soil column. In the case of GW, the largest differences are seen over the northwest of the domain, reaching values larger than $0.12\,m^3\,m^{-3}$. A permanent difference is observed over the southern La Plata (i.e., LOLP), with mean values between 0.02 and $0.04\,m^3\,m^{-3}$. The differences over the SOAM and the monsoon region (i.e., SAMS) have a more visible seasonal cycle, which peaks at the end of the rainy season. This is due to the reduced drainage in the GW simulation. The relative differences over the northwestern part of the domain can be larger than 40% of FD values. Similar values are observed over parts of the southern Amazon and the monsoon region. Over La Plata, the differences in soil moisture between the GW and FD simulations are in the range of 5%–20%. In the case of SIMGM the extra moisture is seen over a larger region of the domain, and with larger values, as a consequence of the much shallower water table.

Time series of the regional averages of soil moisture in the top 2 m from the simulations are shown in Fig. 6. The annual cycle over the Amazon is more regular, while over La Plata the interannual variations are larger than the annual cycle. The time series for the SOAM and the monsoon region (i.e., SAMS) show that the SM2m field lags precipitation by about 1 month (cf. to 2–3 months for the TWS). Note also that the difference between the groundwater and the FD simulations is a smaller fraction of the amplitude of the annual cycle over the Amazon, but a larger fraction over the La Plata basin. For all four

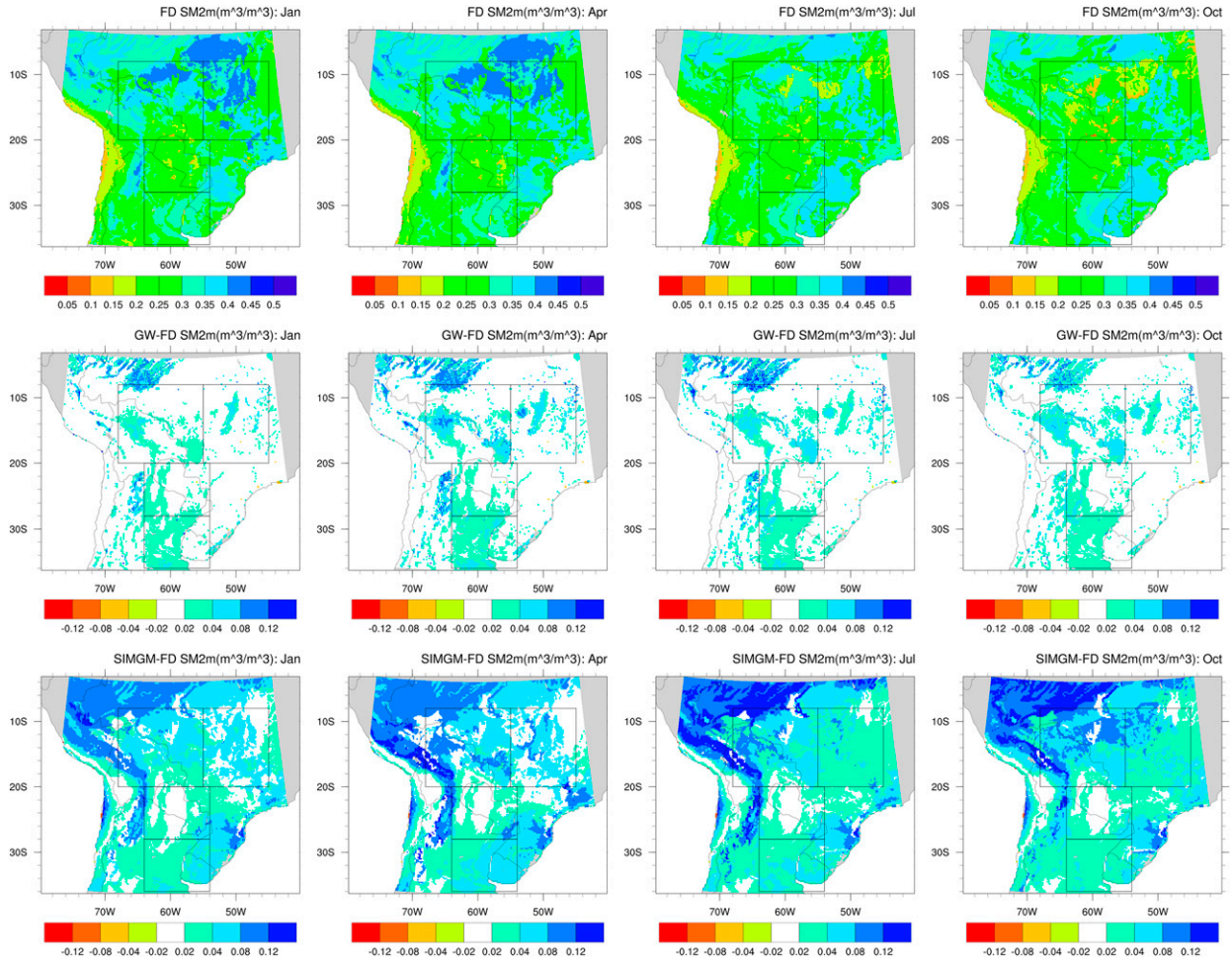

FIG. 5. (top) The SM2m in the FD simulation and absolute differences of (middle) GW − FD and (bottom) SIMGM − FD.

regions, the phase of all time series seems to be the same, in contrast with the TWS fluctuations. Thus, the groundwater scheme is not introducing temporal effects on SM2m in these offline simulations (i.e., where the same atmospheric forcing is used in all simulations). The situation could be different in fully coupled land–atmosphere simulations, where larger values of SM2m in the groundwater simulations could either increase or decrease precipitation (Schär et al. 1999), modifying the surface forcing in magnitude and timing.

Over the southern La Plata (i.e., LOLP) the time series show some interesting features during some of the anomalously dry rainy seasons. One example is the drought between 2008 and 2009. By October 2007, both the GW and FD simulations have relatively similar values of average soil moisture. However, the decrease in soil moisture between October 2007 and February 2008 is larger in the FD simulation, while the groundwater schemes reduce the drainage. Other example is the wet season between 2010 and 2011. The difference in soil moisture between the groundwater and FD simulations is larger in March 2011 than in September 2010. Thus, the FD simulation exhibits a sharper drop in soil moisture as a response to the largest negative anomalies in precipitation. In contrast, large positive anomalies in precipitation can make the moisture in the top 2 m of the soil nearly equal in both the GW and FD simulations, like in the second half of 2012. During those wet events the soil layers closer to the land surface are very moist, contributing more to SM2m, which therefore takes very similar values in both simulations between September and November 2012. However, at the end of the anomalous wet period, the FD simulation dries up faster because of its free drainage boundary condition.

4) EVAPOTRANSPIRATION

Large values of ET are observed over the southeastern part of the domain during the rainy (summer) season (Fig. 7). These values decrease sharply during the dry (winter) season. Around July, ET over the

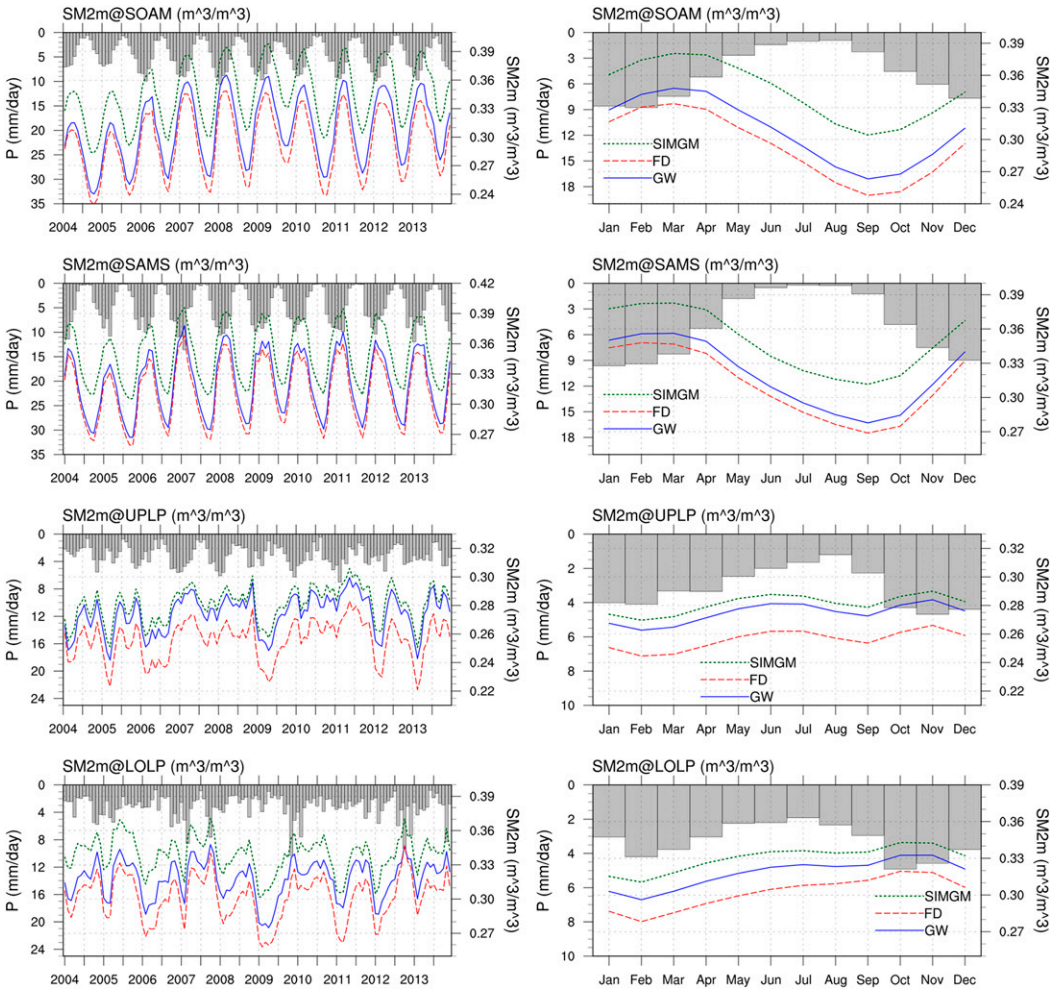

FIG. 6. SM2m (curves) and precipitation (bars) averaged over the regions in Fig. 5.

monsoon region is very low. It is important to point out that no calibration of Noah-MP has been made, which is reflected on the simulated values of different variables. The simulated ET tends to be lower than the ET from ERA-Interim (not shown) over the northeast of the domain during the dry season (where ET is more energy limited). The simulated ET over the Amazon recovers by October.

The groundwater simulations produce more ET than the FD simulation over parts of the La Plata basin and the southern Amazon (Fig. 7), which is a result of moister soils, especially in the SIMGM simulation (Fig. 5). Note that there are no ET differences over the northwestern part of the domain, despite the significant differences in soil moisture (Fig. 5); in that region ET is mostly limited by radiation. The differences over the southern Amazon peak during the dry and before the onset of the rainy seasons, when ET tends to be more water limited. Over the La Plata region the difference in ET is larger at the onset of the rainy season (around October) because of the combination of enough radiation and water available. Over the monsoon region (i.e., our SAMS) the difference in ET has two peaks during the year, around the end and the onset of the rainy season (see Fig. 8 and the time series of the difference in ET below). During the peak of the dry season the difference in ET has a local minimum (as in the case of total ET; see Fig. 7). The largest relative differences between GW and FD are found during the dry season (when absolute ET is smaller), reaching values larger than 40% of the FD values. Note that during the onset (around October) and demise (around April) of the rainy season, the relative differences between GW and FD over the southern La Plata are larger than 10%. Even in the middle of the rainy season (e.g., January), the GW simulations produce around 10% or more ET over the southern La Plata, which could enhance precipitation in coupled simulations. The relative differences

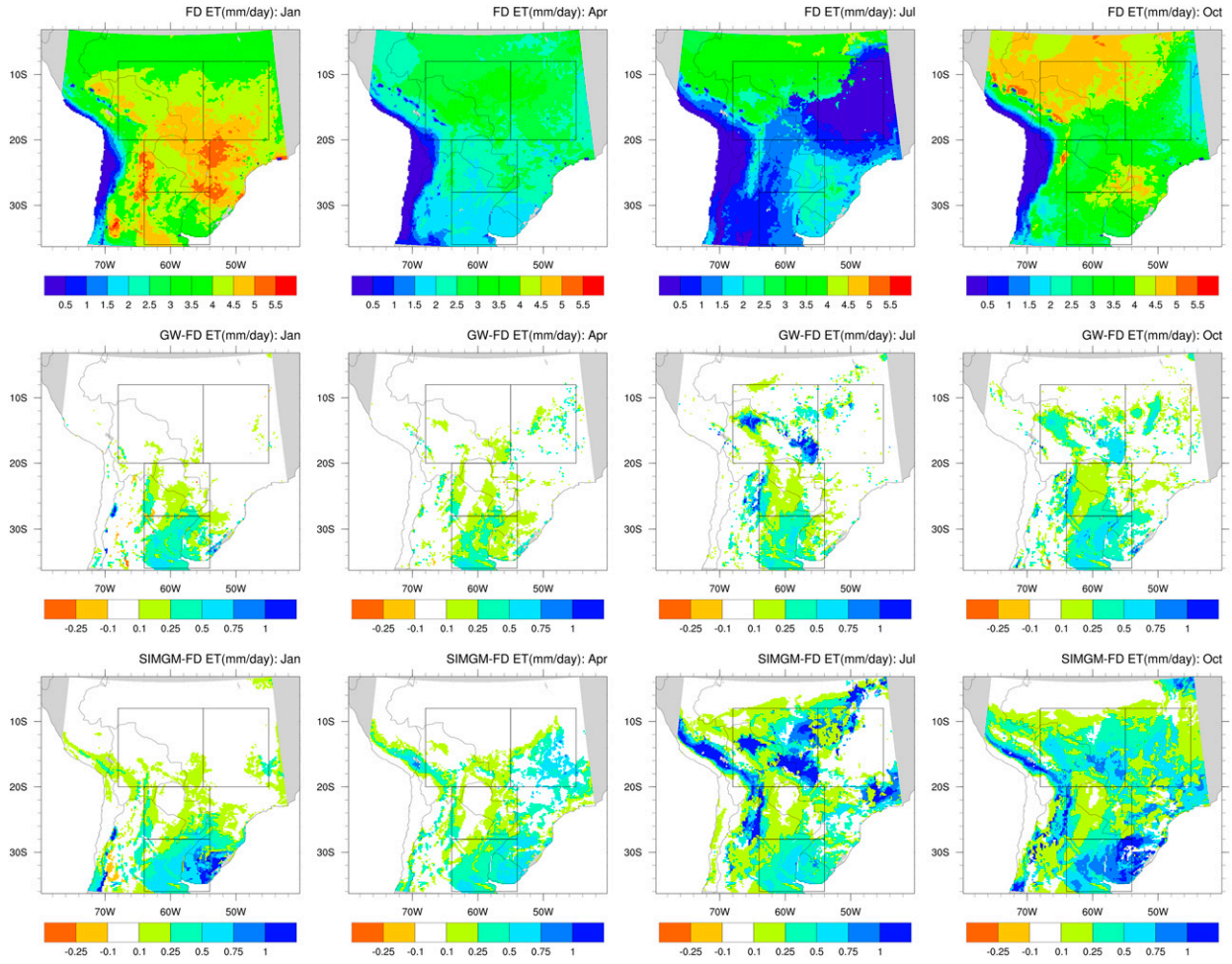

FIG. 7. (top) The ET in the FD simulation and absolute differences of (middle) GW − FD and (bottom) SIMGM − FD.

are even larger and more widespread for the SIMGM simulation.

The regional averages of ET show that the differences between the groundwater and the FD simulations are much smaller than the amplitude of their seasonal cycle (Fig. 8). The phase of the fluctuations is virtually the same in all three simulations for all regions (as in the case of SM2m). For reference, we also plotted the regional averages of ET from the LandFlux–EVAL project (Mueller et al. 2013). The median values (LFE-50) shown in Fig. 8 correspond to the median ET product from all the model- and observation-based estimates gathered in LandFlux–EVAL. In all four subregions the differences between the LandFlux–EVAL estimates and our simulations can be beyond the interquartile range (IQR) in the LandFlux–EVAL merged product, likely due to the lack of calibration of the Noah-MP model with ERA-Interim forcing data. For SOAM, the groundwater simulations produce more ET during the dry season and the first part of the rainy season (June–November), which shows the buffering effect of the groundwater schemes when precipitation decreases. In the case of the monsoon region (SAMS), the regional average from the GW simulation is almost identical to that from the FD simulation, because the differences are limited to a small region and for a limited time during the year (see Fig. 7). A larger difference is observed between the SIMGM and FD simulations, especially around May.

In the case of La Plata, our simulations overestimate ET with respect to LandFlux–EVAL (Fig. 8), with the groundwater simulations producing higher values at the end of the dry (August) season and the early stages of the rainy season (October). The differences (GW − FD) and (SIMGM − FD) are somewhat larger around October–November, but they can be seen throughout the year. The effect of the groundwater schemes on the

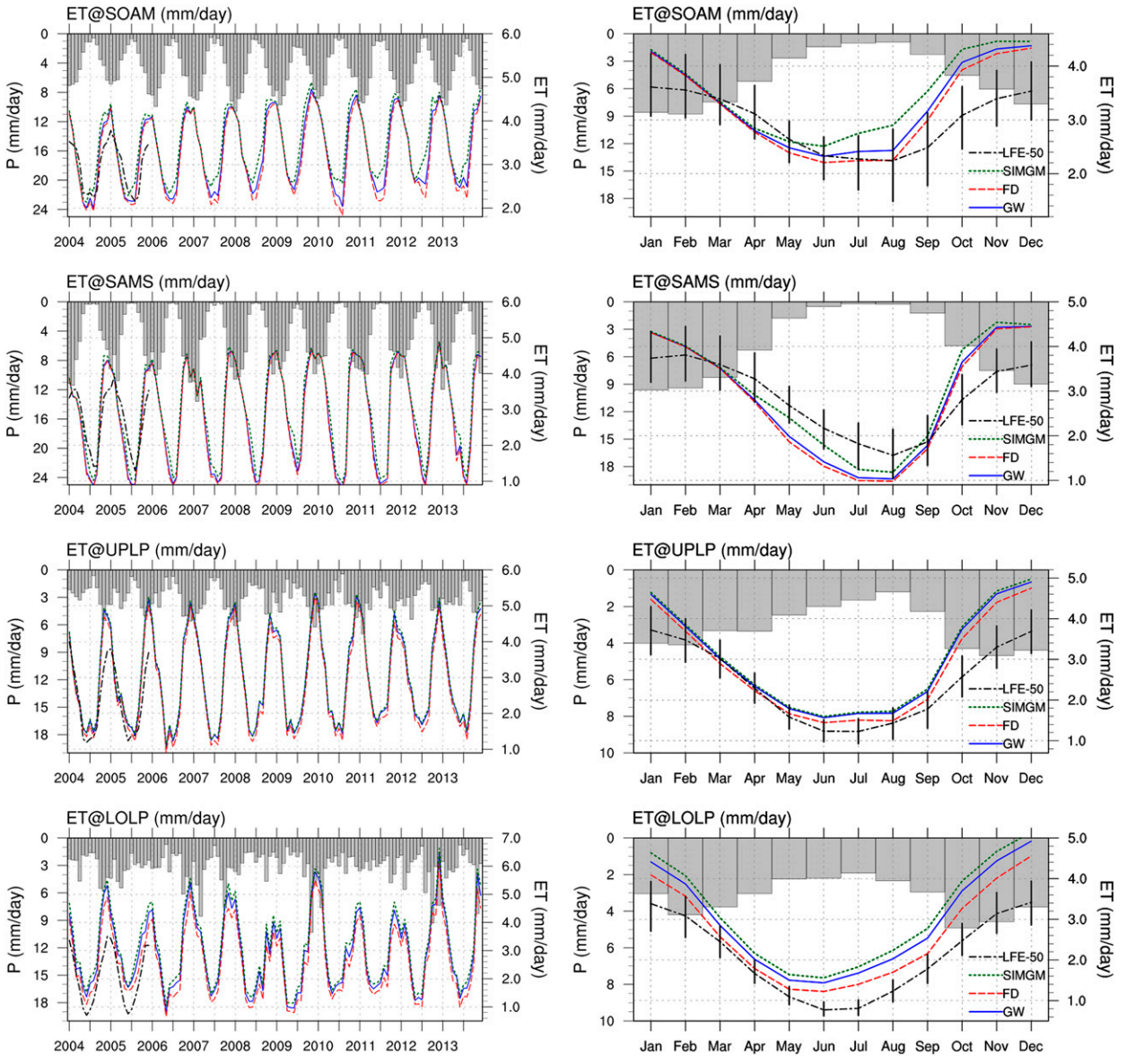

FIG. 8. The ET (curves) and precipitation (bars) averaged over the regions in Fig. 7. LFE-50 represents the median values of the LandFlux–EVAL merged product, with the lower and upper limits of the vertical bars given by the 25th and 75th percentile products. (right) The base period for the long-term mean annual cycle is 1989–2005 for the LandFlux–EVAL product and 2004–13 for the FD, GW, and SIMGM simulations. (left) Monthly estimates from LandFlux–EVAL are shown only for 2004–05 because data are available for 1989–2005.

increase in ET is larger over the southern La Plata (i.e., LOLP).

In general, our simulations show a positive bias in ET with respect to the LandFlux–EVAL product, except for the large negative bias in the SAMS during the dry season (Vinukollu et al. 2011; Jiménez et al. 2011). However, as stated earlier, our focus is the differences introduced by two groundwater schemes within the same LSM, which is Noah-MP in our case. In this sense we find that the differences in ET between the groundwater schemes and the FD simulation are within typical intermodel spread, as suggested by the IQR of the LandFlux–EVAL product and other studies (e.g., Mueller et al. 2011), but in our case the difference is due only to the groundwater scheme of the LSM. This further illustrates the importance of studying the effect of this component for its proper use in the newer LSMs.

b. *Role of the horizontal resolution*

To compare with the 20-km simulations, the ET field from each of the 5-km grid size simulations has been aggregated to the 20-km grid before computing the (GW − FD) fields and their spatial averages. However,

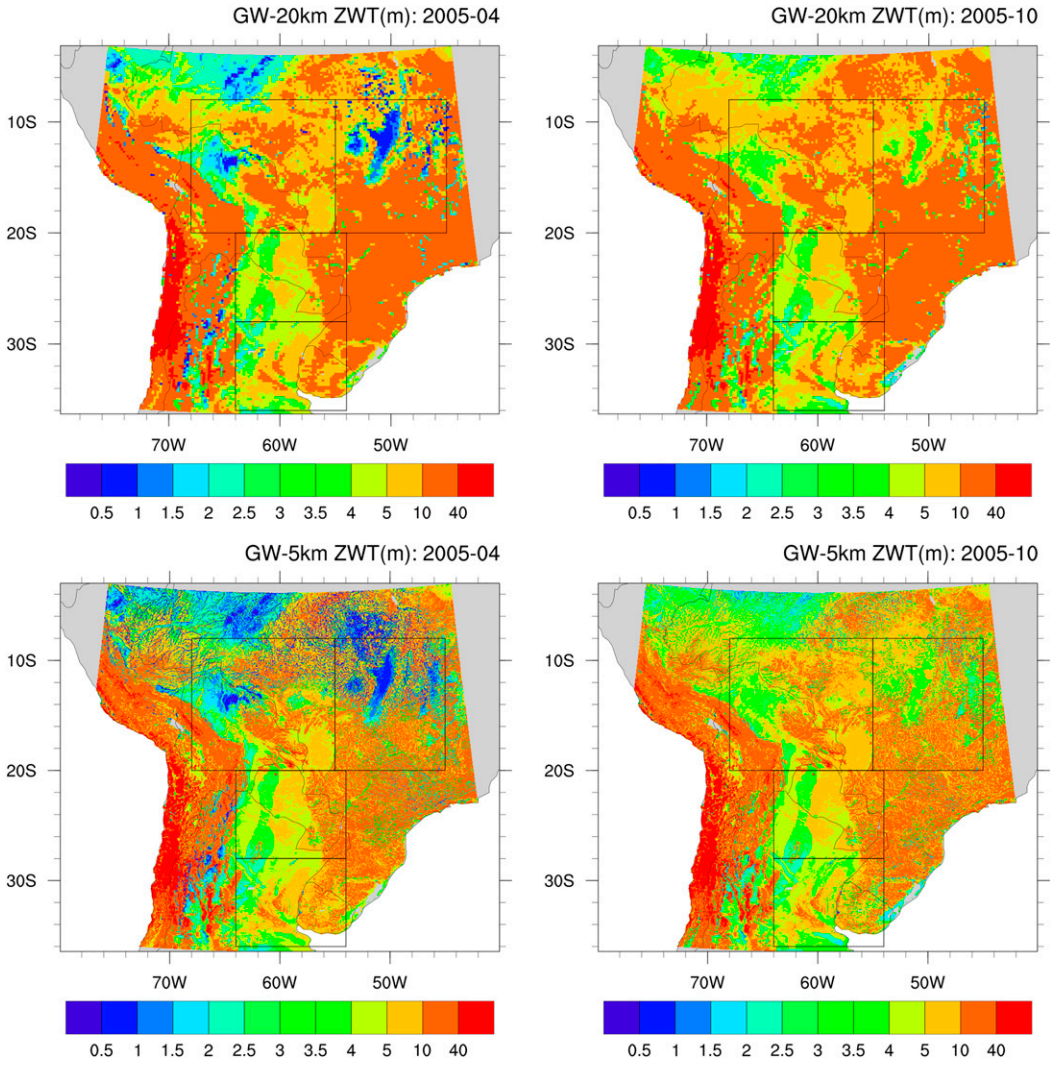

FIG. 9. Depth to water table as simulated by the MMF groundwater scheme in the second year of simulation for grid sizes (top) 20 and (bottom) 5 km. Only results for (left) April and (right) October are shown as they are representative of the largest differences at the extremes of the water-table depth annual cycle (see Fig. 3).

the water-table fields are shown at the original grid size to highlight the effect of the resolution. At higher resolution, finer details of the topographical gradients are captured, which in turn leads to larger lateral flows of groundwater toward local (as opposed to regional) topographic depressions. In turn, this induces shallower water tables over a larger area in the higher-resolution simulation compared with the lower resolution (Fig. 9). This effect, however, is not homogeneous in space, as it is more pronounced where the topographical gradients are larger. In our region of interest, the difference is more noticeable over the north and east of the domain, including the SOAM and the monsoon region (i.e., SAMS). On the contrary, the topographical gradients are smoother in the 20-km simulation, reducing the lateral flow as represented in the MMF groundwater scheme. The differences of the water-table depth over the La Plata region (including UPLP and LOLP) are not as pronounced as over the Amazon, because the small-scale topographical gradients are relatively smaller (see Fig. 1).

As a result of having more grid cells with a shallower water table, the 5-km simulations produce more regions where the groundwater scheme increases ET that are not observed in the 20-km simulations (Fig. 10). For example, during the wet season (January), the 5-km simulation induces an increase in ET over parts of the SOAM, Uruguay, and southern Brazil. By the end of the rainy season (April) over the monsoon region (i.e., SAMS) the groundwater effects in the 5-km simulation are also visible. During the dry season (July), the

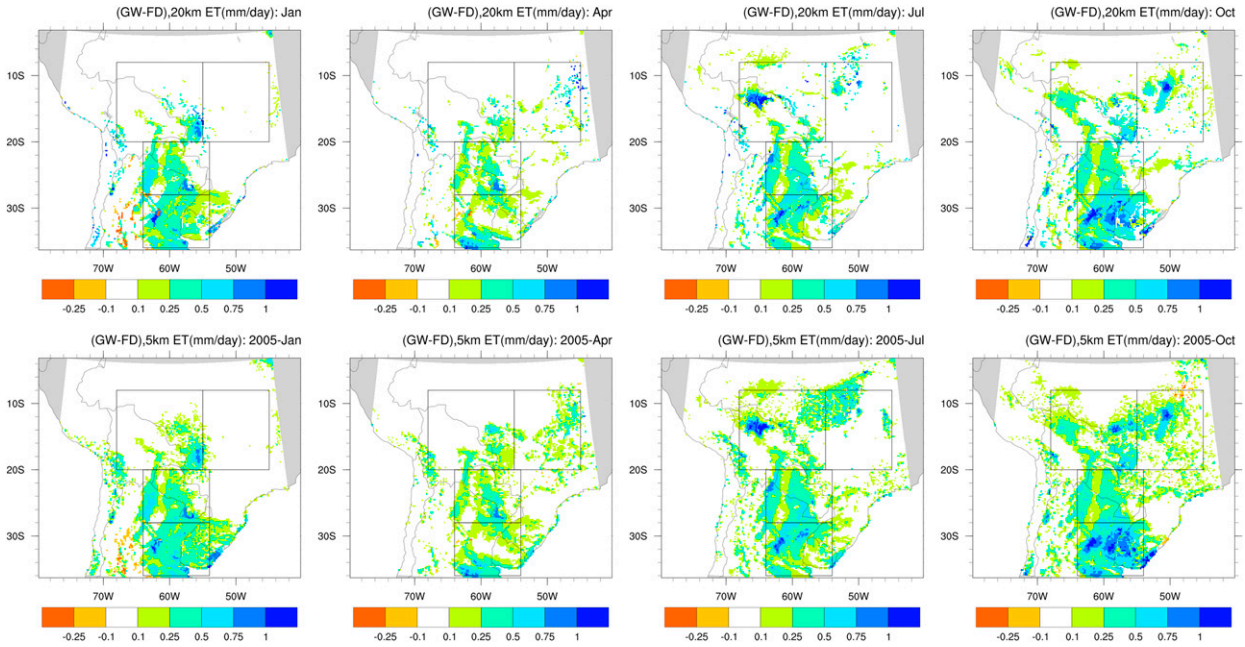

FIG. 10. Difference in ET between the GW and FD simulations in the second year of simulation. Simulation grid sizes are (top) 20 and (bottom) 5 km.

northwest corner of the box representing the monsoon region, and the northeast of the southern Amazon, show an increase in ET, which in the 5-km simulations is greater than 0.5 mm day^{-1}, while a smaller area, with lower values, is observed in the 20-km simulations. During October, the effects of the groundwater scheme over the monsoon region span a larger area in the high-resolution simulation.

For all four regions of interest, the simulations with 5-km grid size show a larger increase in ET (i.e., larger ΔET) due to the groundwater scheme (Fig. 11). During the peak of ΔET, the groundwater scheme plays a major role on ET, and the scale effects are more pronounced because of the existence of a larger area with a shallow water table in the high-resolution simulations. On the contrary, during the peak of the rainy season, the groundwater scheme has a smaller role on ET, and the differences due to resolution are consequently smaller. The horizontal resolution does not introduce differences in the timing of ΔET, but increases its magnitude. The effects of the higher resolution can be very large over disconnected but nearby grid cells, and its widespread distribution is visible even at the regional scale, as seen both from the monthly maps (Fig. 10) and the spatial averages (Fig. 11) of ΔET. In general, the comparison of the 5- and 20-km simulations suggests that the resolution effects of the MMF scheme on ET are neither spatially homogeneous nor negligible at spatial scales relevant to the current use of RCMs for climate simulations at the continental scale. In particular, the regions most affected by the groundwater scheme at higher resolution can span hundreds of kilometers, and the increase in ET can be larger than 1 mm day^{-1}, like in the case of the southern Amazon during the dry season. A difference of this magnitude in the land surface fluxes might have an impact on the simulation of the atmosphere in RCMs, even with a grid size of the order of 20 km, although their land surface model would not be able to capture the groundwater effect in the first place.

4. Summary and discussion

The MMF scheme improves the simulated amplitude of the seasonal cycle of TWS over parts of the Amazon and central-eastern Brazil (i.e., what we call in this paper the monsoon region or SAMS), as compared with GRACE estimates. Pokhrel et al. (2013) also report an improvement in the simulation of the terrestrial water storage over the Amazon region due to the MMF groundwater scheme. Pokhrel et al. (2013) use a much higher resolution (~2 km grid size) compared with this study (20 km). It is therefore interesting to note that the MMF groundwater scheme can improve the simulation of TWS over the Amazon even at grid sizes typical of current continental-scale RCM simulations. Over the La Plata basin, the groundwater schemes induce a larger long-term decline in the TWS, as well as larger monthly fluctuations (like in the case of the drought between 2008 and 2009; see Fig. 4). A larger long-term decline in

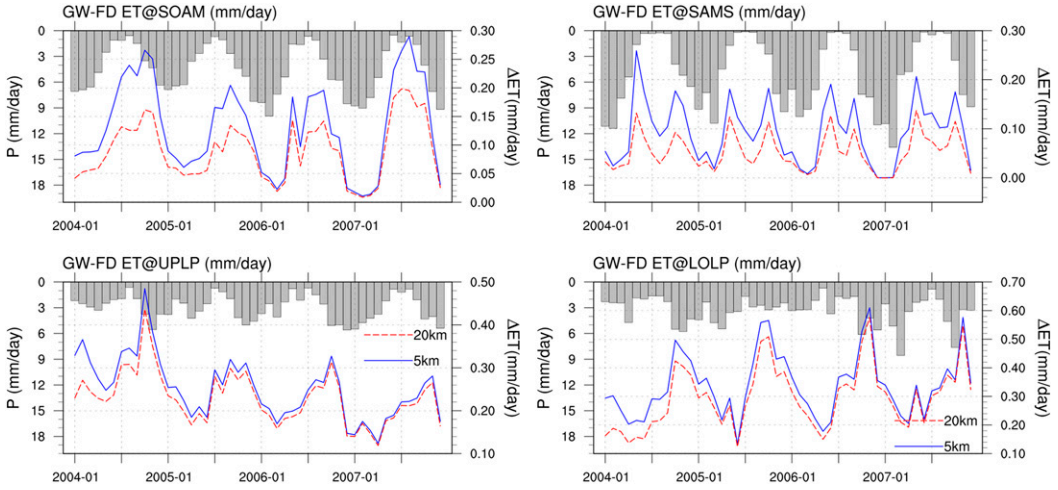

FIG. 11. Difference in ET between the GW and FD simulations in the second year of simulation. The blue (red) curve shows the difference in ET for simulations with grid size of 5 km (20 km). Simulation grid sizes are (top) 20 and (bottom) 5 km.

the TWS was also reported by Chen et al. (2010) for the southern La Plata, both from GRACE and groundwater observations, when compared with GLDAS-Noah (which has no groundwater scheme).

The groundwater schemes also induce an increase in the simulated moisture in the top 2 m of the soil over those regions where the water table is closer to the surface. Over the northwest of the domain, the smallest increase was obtained with the MMF scheme, and it can be as large as 40%. Over parts of the southern Amazon, the monsoon region, and the La Plata basin, the increase in soil moisture is larger than 5%–20%. The increase in soil moisture in the top 2 m (the root zone of the model) in turn induces an increase of evapotranspiration, but mostly over those regions/seasons where ET is more water limited. This is the case for the southern La Plata (throughout the year) and parts of the southern Amazon and the monsoon region (between the dry and the onset of the rainy seasons). When the increase in ET takes place in regions where the water table is within the rooting depth, part of the extra ET comes from direct uptake of moisture from the saturated layers below the water table (i.e., direct groundwater uptake) and within the reach of the roots. In particular, during the onset and demise of the rainy season over the La Plata basin, the MMF groundwater scheme can increase ET on the order of 10%, which might have an impact on precipitation recycling in fully coupled simulations. This effect could be even larger with the SIMGM scheme.

Comparison of simulations with grid sizes of 20 and 5 km show that the latter depict significantly more grid cells where the water table is shallower, impacting ET over a larger area. The most dramatic effects are observed over parts of the southern Amazon and the monsoon region. A more rigorous assessment of the role of the horizontal resolution requires separate spinup stages for the 5- and 20-km grid size simulations, in order for the models to reach their individual equilibrium states. However, the similarities between the short and the long 20-km simulations (cf. Fig. 10 to Fig. 7), in addition to the steady character observed in the comparison of the short 20- and 5-km simulations (Fig. 11), suggests that our results provide a good idea of the true effects of the groundwater scheme at different resolutions.

It is important to note that the lateral flow of groundwater is expected to be relatively small at 20 and even at 5 km. However, the vertical exchange within the soil layers is still important for the soil moisture budget. Therefore, a significant part of the effects of the MMF groundwater scheme found in this study are due to the initial and equilibrium states of the water table, which were found from much higher-resolution computations (~270 m) in previous studies (Fan and Miguez-Macho 2010). This water-table distribution is realistic (Fan et al. 2013), which is expected to induce realistic effects on the soil moisture and ET fields even at the resolutions of the present study, thus providing a novel result compared with idealized experiments reported elsewhere (e.g., Collini et al. 2008). Despite the coarse resolution used for the lateral flow in this study, there is an important difference in the simulations at 20 and 5 km, as discussed above.

The present study is intended to be a contribution to the general understanding of the effect of a groundwater scheme on the simulation of the hydrological cycle over part of South America, in the context of climate studies. In particular, the La Plata basin has been identified as a

region where a groundwater scheme could induce significant impacts on the simulation of the soil moisture and evapotranspiration. In our simulations, the impacts of the MMF groundwater scheme on soil moisture and ET are larger than those reported by Niu et al. (2007) and Koirala et al. (2014). However, the impact could be even larger if the simulated water table would have the same shallow profile as estimated by Fan and Miguez-Macho (2010) and Fan et al. (2013), and as found with the SIMGM scheme. In general, there is a critical need for studying and optimizing the sophisticated LSMs that are available now (see, e.g., Getirana et al. 2014), in particular when including components like groundwater schemes, which have a region-dependent impact on the simulation of land states and fluxes. As discussed by Miguez-Macho and Fan (2012b), the real impact of shallow groundwater on the hydrologic systems of South America has to be assessed via field measurements and a more detailed representation of the soil characteristics in LSMs. Our study suggests that, taking into account the strong coupling of surface conditions and precipitation over the La Plata basin (Sörensson and Menéndez 2011), a groundwater scheme could also impact the simulation of the rainy season in climate simulations, including the precipitation recycling during droughts. This is the focus of our companion paper (Martinez et al. 2016).

Acknowledgments. We acknowledge the Research Applications Laboratory (RAL) from NCAR–UCAR for providing the Noah-MP code on their website http://www.ral.ucar.edu/research/land/technology/noahmp_lsm.php. We also acknowledge Dr. Michael Barlage at NCAR for providing support to install and run the model. We acknowledge the ECMWF for providing the ERA-Interim data, GRCTellus for providing the GRACE data, and Landflux.org for providing the ET estimates. GRACE land data are available at http://grace.jpl.nasa.gov, supported by the NASA MEaSUREs Program. We also acknowledge the Land–Climate Dynamics Group at ETH for providing the LandFlux–EVAL data (http://www.iac.ethz.ch/group/land-climate-dynamics/research/landflux-eval.html). We are grateful to James Shuttleworth and Hoshin Gupta for their insightful comments. We also acknowledge the comments and suggestions from the reviewers for helping to improve the present work. This research was supported by NSF Grant AGS 1045260 and NSF CAREER Award AGS 1454089 (Martinez and Dominguez) and by the European Commission FP7 "EartH2Observe" project (Miguez-Macho).

REFERENCES

Anyah, R. O., C. P. Weaver, G. Miguez-Macho, Y. Fan, and A. Robock, 2008: Incorporating water table dynamics in climate modeling: 3. Simulated groundwater influence on coupled land–atmosphere variability. *J. Geophys. Res.*, **113**, D07103, doi:10.1029/2007JD009087.

Barlage, M., M. Tewari, F. Chen, G. Miguez-Macho, Z.-L. Yang, and G.-Y. Niu, 2015: The effect of groundwater interaction in North American regional climate simulations with WRF/Noah-MP. *Climatic Change*, **129**, 485–498, doi:10.1007/s10584-014-1308-8.

Berbery, E. H., and V. R. Barros, 2002: The hydrologic cycle of the La Plata basin in South America. *J. Hydrometeor.*, **3**, 630–645, doi:10.1175/1525-7541(2002)003<0630:THCOTL>2.0.CO;2.

Betts, A. K., M. Köhler, and Y. Zhang, 2009: Comparison of river basin hydrometeorology in ERA-Interim and ERA-40 reanalyses with observations. *J. Geophys. Res.*, **114**, D02101, doi:10.1029/2008JD010761.

Chen, J. L., C. R. Wilson, B. D. Tapley, L. Longuevergne, Z. L. Yang, and B. R. Scanlon, 2010: Recent La Plata basin drought conditions observed by satellite gravimetry. *J. Geophys. Res.*, **115**, D22108, doi:10.1029/2010JD014689.

Collini, E. A., E. H. Berbery, V. R. Barros, and M. E. Pyle, 2008: How does soil moisture influence the early stages of the South American monsoon? *J. Climate*, **21**, 195–213, doi:10.1175/2007JCLI1846.1.

Dee, D. P., and Coauthors, 2011: The ERA-Interim reanalysis: Configuration and performance of the data assimilation system. *Quart. J. Roy. Meteor. Soc.*, **137**, 553–597, doi:10.1002/qj.828.

Dirmeyer, P. A., C. A. Schlosser, and K. L. Brubaker, 2009: Precipitation, recycling, and land memory: An integrated analysis. *J. Hydrometeor.*, **10**, 278–288, doi:10.1175/2008JHM1016.1.

Fan, Y., 2015: Groundwater in the Earth's critical zone: Relevance to large-scale patterns and processes. *Water Resour. Res.*, **51**, 3052–3069, doi:10.1002/2015WR017037.

——, and G. Miguez-Macho, 2010: Potential groundwater contribution to Amazon evapotranspiration. *Hydrol. Earth Syst. Sci.*, **14**, 2039–2056, doi:10.5194/hess-14-2039-2010.

——, H. Li, and G. Miguez-Macho, 2013: Global patterns of groundwater table depth. *Science*, **339**, 940–943, doi:10.1126/science.1229881.

Ferreira, L., H. Salgado, C. Saulo, and E. Collini, 2011: Modeled and observed soil moisture variability over a region of Argentina. *Atmos. Sci. Lett.*, **12**, 334–339, doi:10.1002/asl.342.

Getirana, A. C. V., and Coauthors, 2014: Water balance in the Amazon basin from a land surface model ensemble. *J. Hydrometeor.*, **15**, 2586–2614, doi:10.1175/JHM-D-14-0068.1.

Jiménez, C., and Coauthors, 2011: Global intercomparison of 12 land surface heat flux estimates. *J. Geophys. Res.*, **116**, D02102, doi:10.1029/2010JD014545.

Koirala, S., P. J.-F. Yeh, Y. Hirabayashi, S. Kanae, and T. Oki, 2014: Global-scale land surface hydrologic modeling with the representation of water table dynamics. *J. Geophys. Res. Atmos.*, **119**, 75–89, doi:10.1002/2013JD020398.

Koster, R. D., Z. Guo, R. Yang, P. A. Dirmeyer, K. Mitchell, and M. J. Puma, 2009: On the nature of soil moisture in land surface models. *J. Climate*, **22**, 4322–4335, doi:10.1175/2009JCLI2832.1.

Kuppel, S., J. Houspanossian, M. D. Nosetto, and E. G. Jobbágy, 2015: What does it take to flood the Pampas?: Lessons from a decade of strong hydrological fluctuations. *Water Resour. Res.*, **51**, 2937–2950, doi:10.1002/2015WR016966.

Landerer, F. W., and S. C. Swenson, 2012: Accuracy of scaled GRACE terrestrial water storage estimates. *Water Resour. Res.*, **48**, W04531, doi:10.1029/2011WR011453.

Lee, S.-J., and E. H. Berbery, 2012: Land cover change effects on the climate of the La Plata basin. *J. Hydrometeor.*, **13**, 84–102, doi:10.1175/JHM-D-11-021.1.

Marengo, J. A., W. R. Soares, C. Saulo, and M. Nicolini, 2004: Climatology of the low-level jet east of the Andes as derived from the NCEP–NCAR reanalyses: Characteristics and

temporal variability. *J. Climate*, **17**, 2261–2280, doi:10.1175/1520-0442(2004)017<2261:COTLJE>2.0.CO;2.

——, and Coauthors, 2012: Recent developments on the South American monsoon system. *Int. J. Climatol.*, **32**, 1–21, doi:10.1002/joc.2254.

Martinez, J. A., and F. Dominguez, 2014: Sources of atmospheric moisture for the La Plata River basin. *J. Climate*, **27**, 6737–6753, doi:10.1175/JCLI-D-14-00022.1.

——, ——, and G. Miguez-Macho, 2016: Impacts of a groundwater scheme on hydrometeorological conditions over southern South America. *J. Hydrometeor.*, **17**, 2959–2978, doi:10.1175/JHM-D-16-0052.1.

Miguez-Macho, G., and Y. Fan, 2012a: The role of groundwater in the Amazon water cycle: 1. Influence on seasonal streamflow, flooding and wetlands. *J. Geophys. Res.*, **117**, D15113, doi:10.1029/2012JD017539.

——, and ——, 2012b: The role of groundwater in the Amazon water cycle: 2. Influence on seasonal soil moisture and evapotranspiration. *J. Geophys. Res.*, **117**, D15114, doi:10.1029/2012JD017540.

——, ——, C. P. Weaver, R. Walko, and A. Robock, 2007: Incorporating water table dynamics in climate modeling: 2. Formulation, validation, and soil moisture simulation. *J. Geophys. Res.*, **112**, D13108, doi:10.1029/2006JD008112.

Mueller, B., and Coauthors, 2011: Evaluation of global observations based evapotranspiration datasets and IPCC AR4 simulations. *Geophys. Res. Lett.*, **38**, L06402, doi:10.1029/2010GL046230.

——, and Coauthors, 2013: Benchmark products for land evapotranspiration: LandFlux–EVAL multi-data set synthesis. *Hydrol. Earth Syst. Sci.*, **17**, 3707–3720, doi:10.5194/hess-17-3707-2013.

Müller, O. V., E. H. Berbery, D. Alcaraz-Segura, and M. B. Ek, 2014: Regional model simulations of the 2008 drought in South America using a consistent set of land surface properties. *J. Climate*, **27**, 6754–6778, doi:10.1175/JCLI-D-13-00463.1.

Niu, G.-Y., Z.-L. Yang, R. E. Dickinson, L. E. Gulden, and H. Su, 2007: Development of a Simple Groundwater Model for use in climate models and evaluation with Gravity Recovery and Climate Experiment data. *J. Geophys. Res.*, **112**, D07103, doi:10.1029/2006JD007522.

——, and Coauthors, 2011: The community Noah land surface model with multiparameterization options (Noah-MP): 1. Model description and evaluation with local-scale measurements. *J. Geophys. Res.*, **116**, D12109, doi:10.1029/2010JD015139.

Pfeffer, J., and Coauthors, 2014: Low-water maps of the groundwater table in the central Amazon by satellite altimetry. *Geophys. Res. Lett.*, **41**, 1981–1987, doi:10.1002/2013GL059134.

Pokhrel, Y. N., Y. Fan, G. Miguez-Macho, P. J.-F. Yeh, and S.-C. Han, 2013: The role of groundwater in the Amazon water cycle: 3. Influence on terrestrial water storage computations and comparison with GRACE. *J. Geophys. Res. Atmos.*, **118**, 3233–3244, doi:10.1002/jgrd.50335.

Rawitscher, F., 1948: The water economy of the vegetation of the 'Campos Cerrados' in Southern Brazil. *J. Ecol.*, **36**, 237–268, doi:10.2307/2256669.

Rodell, M., and Coauthors, 2004: The Global Land Data Assimilation System. *Bull. Amer. Meteor. Soc.*, **85**, 381–394, doi:10.1175/BAMS-85-3-381.

Schär, C., D. Lüthi, and U. Beyerle, 1999: The soil–precipitation feedback: A process study with a regional climate model. *J. Climate*, **12**, 722–741, doi:10.1175/1520-0442(1999)012<0722:TSPFAP>2.0.CO;2.

Solman, S. A., and Coauthors, 2013: Evaluation of an ensemble of regional climate model simulations over South America driven by the ERA-Interim reanalysis: Model performance and uncertainties. *Climate Dyn.*, **41**, 1139–1157, doi:10.1007/s00382-013-1667-2.

Sörensson, A. A., and C. G. Menéndez, 2011: Summer soil–precipitation coupling in South America. *Tellus*, **63A**, 56–68, doi:10.1111/j.1600-0870.2010.00468.x.

——, and E. H. Berbery, 2015: A note on soil moisture memory and interactions with surface climate for different vegetation types in the La Plata basin. *J. Hydrometeor.*, **16**, 716–729, doi:10.1175/JHM-D-14-0102.1.

Swenson, S. C., and J. Wahr, 2006: Post-processing removal of correlated errors in GRACE data. *Geophys. Res. Lett.*, **33**, L08402, doi:10.1029/2005GL025285.

Tomasella, J., M. G. Hodnett, L. A. Cuartas, A. D. Nobre, M. J. Waterloo, and S. M. Oliveira, 2008: The water balance of an Amazonian micro-catchment: The effect of inter-annual variability of rainfall on hydrological behaviour. *Hydrol. Processes*, **22**, 2133–2147, doi:10.1002/hyp.6813.

Vera, C., and Coauthors, 2006: Toward a unified view of the American monsoon systems. *J. Climate*, **19**, 4977–5000, doi:10.1175/JCLI3896.1.

Vinukollu, R. K., R. Meynadier, J. Sheffield, and E. Wood, 2011: Multi-model, multi-sensor estimates of global evapotranspiration: Climatology, uncertainties and trends. *Hydrol. Processes*, **25**, 3993–4010, doi:10.1002/hyp.8393.